Astron. Astrophys. 322, 674–678 (1997)

ASTRONOMY
AND
ASTROPHYSICS

Lyman continuum as a diagnostic for nonthermal processes in solar flares

M.D. Ding[1,2] **and H. Schleicher**[1]

[1] Kiepenheuer-Institut für Sonnenphysik, Schöneckstr. 6, D-79104 Freiburg, Germany
[2] Department of Astronomy, Nanjing University, Nanjing 210093, China

Received 9 September 1996 / Accepted 15 November 1996

Abstract. We have computed the Lyman continuum intensities for different flare circumstances, namely, the temperature rise in the chromosphere, the downward shift of the transition region, and the nonthermal effect of a precipitating beam of electrons. All the three factors can enhance the intensity by various amounts. The third effect additionally lowers the color temperature of the Lyman continuum. It thus provides a diagnostic tool to discriminate whether there exists an obvious nonthermal effect of electron beam bombardment during solar flares. It is also suggested that the relative magnitudes of Lyman and Balmer continuum enhancements can be used to infer the energy distribution type of the beam electrons.

Key words: Sun: chromosphere – Sun: flares – Sun: UV radiation

1. Introduction

It is now widely accepted that the atmosphere in solar flares is heated by either nonthermal particle bombardment or heat conduction from the corona where the energy is originally released. The type of energy transport process determines directly the spectral signatures in line and continuum emissions. In this respect, the nonthermal effect of electron beam bombardment has attracted much attention since nonthermal electrons are believed to be associated with flare hard X-ray or microwave bursts which have been frequently observed (see e.g., Thompson et al. 1992). Numerical calculations have been performed for line profiles (Fang et al. 1993; Hénoux et al. 1995) and the visible continuum (Aboudarham & Hénoux 1987; Aboudarham et al. 1990; Hénoux et al. 1990) emergent from an electron-beam bombarded atmosphere.

In contrast, the Lyman continuum (Lc) emission has been less tackled. Available observations have shown that the Lc is greatly enhanced relative to the quiet-Sun and attains values with orders of magnitude differences from flare to flare (e.g., Machado & Noyes 1978; Machado et al. 1980). In the near future, we can anticipate that more spectral observations covering the EUV band will appear owing to the recent space programs. Therefore, it seems to be quite desirable to investigate how the Lc varies with different flare-associated atmospheric disturbances and, in particular, its possible role in diagnosing the nonthermal processes in solar flares.

It is known that the Lc is formed in the upper chromosphere and lower transition region (Avrett 1991). So it is much more sensitive to the flare processes than the Balmer continuum (Bc) or Paschen continuum (Pc) which are formed in deeper layers. Moreover, in the wavelength region closely shortward of the Lyman jump, the recombination of hydrogen atoms is the most dominant emission process (Vernazza & Noyes 1972). This is an advantage compared to the visible continuum which is sometimes rather ambiguous as to whether H_{fb} or H^- (negative hydrogen ions) emission is the main contributor (Fang & Ding 1995). With the purpose stated above, we organize the paper as follows: the numerical method and results are displayed in Sect. 2, some discussions are made in Sect. 3, while a brief summary is given in Sect. 4.

2. Numerical method and results

2.1. General procedure

In order to compute the Lc from an atmosphere, we must treat the full non-LTE problem, that is, to solve iteratively the equations describing the radiative transfer, statistical equilibrium, hydrostatic equilibrium, and particle conservation. Particularly, when the atmosphere is bombarded by an electron beam, the deposited energy causes nonthermal excitation and ionization of the hydrogen atoms. The rates of these nonthermal collisional transitions are to be added to the radiative and thermal collisional rates in the statistical equations. A four-level-plus-continuum atomic model for hydrogen is adopted here. The method is similar to that of Fang et al. (1993), where a detailed description about the energy deposition rate and the nonthermal collisional excitation and ionization rates is presented.

Send offprint requests to: H. Schleicher

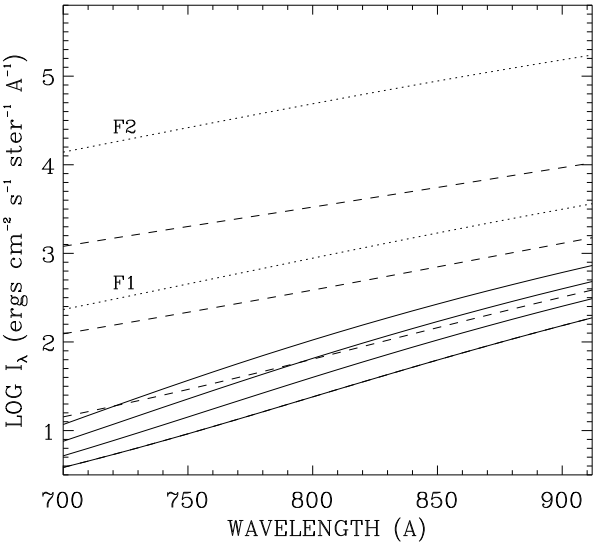

Fig. 1. Lyman continuum intensities at the disk center computed for various atmospheric models showing the effects of varying chromospheric temperatures and top column mass densities. From bottom to top, solid lines correspond to $\Delta T_{\rm top}$ = 0, 1000, 2000, and 3000 K, while dashed lines to $m_{\rm top}$ = 7.4 10^{-6}, 3.0 10^{-5}, 3.0 10^{-4}, and 3.0 10^{-3} g cm^{-2}. Notice the overlapping of the lowest solid and dashed lines (quiet-Sun case). The two dotted lines correspond to flare models F1 (the lower one) and F2 (the upper one). See text for details

To study the Lc signatures under different flare processes, we modify the model atmosphere in a parametrized way. Based on the results of semiempirical flare models, it is known that their most significant modifications relative to the quiet-Sun model are both a temperature rise in the upper chromosphere and a downward shift of the transition region, which may result from the evaporation of chromospheric material into the corona (see e.g., Gan & Fang 1987). In what follows, we consider these two processes and the nonthermal effect independently to show what kinds of Lc emissions would be produced respectively. It should be mentioned that, solar flares certainly involve a drastic change of the coronal temperature structure, but it has little influence on the Lc emission as the hydrogen atoms are fully ionized there. Therefore, we will not discuss this issue here.

2.2. *Effect of chromospheric temperature rise*

We start from the quiet-Sun model VAL-C presented by Vernazza et al. (1981) and later modified by Avrett et al. (1984). The flare-induced temperature rise ΔT in the chromosphere is assumed to reach a maximum value $\Delta T_{\rm top}$ at the top chromosphere, decrease downwards linearly with $\log m$, and vanish at the temperature minimum region (TMR), i.e., $\Delta T = \Delta T_{\rm top} \log(m_{\rm min}/m)/\log(m_{\rm min}/m_{\rm top})$, where $m_{\rm top}$ and $m_{\rm min}$ represent the column mass densities at the top chromosphere and the TMR, respectively. Under such circumstances, we have calculated the Lc intensities at the disk center for models with various values of $\Delta T_{\rm top}$, namely, 0, 1000, 2000, and 3000 K. The results are shown in Fig. 1 (solid lines). Note that $\Delta T_{\rm top}$ = 0 is exactly the quiet-Sun case while $\Delta T_{\rm top}$ = 3000 K corresponds roughly to a strong chromospheric flare.

From Fig. 1, it is easily found that the chromospheric temperature rise tends to increase the absolute Lc intensity, as expected. However, the effect of varying $\Delta T_{\rm top}$ seems not to be large. Moreover, there is no obvious difference in the gradients of the four curves, i.e., the derivatives of the logarithmic intensity with respect to wavelength. This means that the color temperature of the spectrum is not changed significantly irrespective of the actual temperature rise in the chromosphere.

2.3. *Effect of transition region shift*

To show the effect of the downward shift of the transition region, we fix the T versus $m - m_{\rm top}$ relation and only vary the values of $m_{\rm top}$. The results are superimposed in Fig. 1 by dashed lines for cases of $m_{\rm top}$ = 7.4 10^{-6}, 3.0 10^{-5}, 3.0 10^{-4}, and 3.0 10^{-3} g cm^{-2}. Again, the first and last cases correspond to the quiet-Sun and a strong flare, respectively.

It is shown that a larger $m_{\rm top}$ also increases the Lc intensity and its effect is more pronounced than the effect of a pure temperature rise. Besides this fact, the larger the $m_{\rm top}$ value, the smaller the curve gradient, implying a higher color temperature of the spectrum.

A realistic flare model should incorporate the above two processes. For comparison, we also plot in Fig. 1 by dotted lines the results for flare models F1 and F2 from Machado et al. (1980), which clearly show a combination of both effects of the temperature rise and the transition region shift. Note that our computed Lc intensities for models F1 and F2 are consistent with the results given by Avrett et al. (1986), although different computation codes have been used.

2.4. *Effect of nonthermal electron beam bombardment*

Now we turn to the case when there exists a precipitating electron beam causing nonthermal excitation and ionization of the hydrogen atoms. We assume a power law distribution for the energy spectrum of the beam electrons with a lower energy cut-off at 20 keV. The Lc intensities are then computed for the quiet-Sun model imposed by electron beams with various energy fluxes $\mathscr{F}$ = 0, 10^{10}, 10^{11}, and 10^{12} ergs cm^{-2} s^{-1}, and various power indices δ = 3, 4, and 5. The zero-flux case just corresponds to the quiet-Sun without including the nonthermal effect. Fig. 2 displays the results.

It is shown that the effect of nonthermal excitation and ionization caused by the electron beam greatly enhances the Lc. The most noticeable phenomenon is that the curve gradient tends to increase significantly with increasing energy fluxes. Therefore, a lower color temperature should be detected if there exist such nonthermal effects. For a quantitative comparison, we have further computed the color temperatures from the resulting spectra at λ = 800 Å, which are shown to be 8760, 7150, 6680, and 6470 K, corresponding to the four cases of $\mathscr{F}$ = 0, 10^{10}, 10^{11}, and 10^{12} ergs cm^{-2} s^{-1} with δ = 4. Color temperatures for the

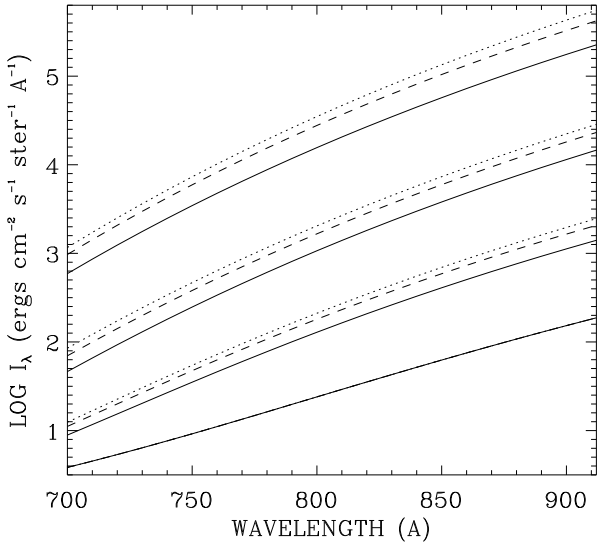

Fig. 2. Lyman continuum intensities at disk center computed for the quiet-Sun model imposed by various electron beams showing the effects of varying their energy fluxes and power indices. Solid, dashed, and dotted lines represent cases of δ = 3, 4, and 5 respectively. From bottom to top, each group of lines correspond to $\mathscr{F}$ = 0, 10^{10}, 10^{11}, and 10^{12} ergs cm^{-2} s^{-1}. Notice the overlapping of the lowest three lines for $\mathscr{F}$ = 0 (quiet-Sun case without any nonthermal effect)

spectra of models F1 and F2 without any nonthermal effect are about 11500 and 12220 K respectively.

One can also find that the energy flux is the main factor determining the enhancement of the Lc intensity. Comparatively, the effect of varying the power index is less pronounced though also very clear. We will further discuss this problem in Sect. 3.

3. Discussions

For the Lc, the Eddington-Barbier relation is a good approximation (Noyes & Kalkofen 1970; Vernazza & Noyes 1972). At the Lc forming layer, the temperature is around 10^4 K, leading to $hc/\lambda kT \gg 1$. Therefore, the Lc intensity can be written as (e.g., Vernazza & Noyes 1972)

$$I_\lambda \approx S_\lambda(T) \approx \frac{B_\lambda(T)}{b_1} \approx \frac{1}{b_1}\frac{2hc^2}{\lambda^5}\mathrm{e}^{-hc/\lambda kT} , \quad (1)$$

where b_1 is the departure coefficient of the hydrogen ground level and T is the temperature at $\tau_\lambda = \mu = \cos\theta$, θ being the angle between the line of sight and the solar vertical. The logarithm of Eq. (1) is

$$\ln I_\lambda \approx \ln\left(\frac{2hc^2}{b_1}\right) - 5\ln\lambda - \frac{hc}{\lambda kT} , \quad (2)$$

and its derivative with respect to wavelength has the form

$$\frac{\mathrm{d}\ln I_\lambda}{\mathrm{d}\lambda} \approx \frac{1}{\lambda}\left(\frac{hc}{\lambda kT} - 5\right) + \left(\frac{hc}{\lambda kT^2}\frac{\mathrm{d}T}{\mathrm{d}\lambda} - \frac{1}{b_1}\frac{\mathrm{d}b_1}{\mathrm{d}\lambda}\right) . \quad (3)$$

It is difficult to evaluate exactly the second term on the right side of Eq. (3), as $b_1(\tau_\lambda = \mu)$ and $T(\tau_\lambda = \mu)$ depend only implicitly on λ. However, approximate estimates show that it is much smaller than the first term in most cases. Equation (3) gives us a rough relation between the gradient of the curves plotted in Figs. 1 and 2 and the temperature in the Lc forming region.

On the basis stated above, it is very easy to explain the general features of the computational results in Sect. 2. When the transition region is shifted downwards, the upper chromosphere is compressed and a larger electron density is produced there, which enhances the Lc opacity and elevates the Lc forming layer (in the reference system of $m - m_{\rm top}$). Thus the spectrum shows a higher color temperature. On the other hand, when the chromospheric temperature is raised while the $m_{\rm top}$ value is kept unchanged, the hydrogen ground level will be less populated and it makes the Lc formed slightly deeper. This mitigates the temperature rise effect to some extent and thus the Lc color temperature is relatively insensitive to $\Delta T_{\rm top}$. Finally, in the case of electron beam bombardment, the predominance of nonthermal excitation and ionization greatly reduces the hydrogen ground level populations, and therefore the Lc is formed in a relatively deeper layer where the temperature is significantly lower than that in the case without any nonthermal effect. As an example, we find that the layer of τ_λ = 1 at λ = 800 Å has a column mass density $\sim$ 3.5 10^{-5} g cm^{-2} for the $\mathscr{F}$ = 10^{11} ergs cm^{-2} s^{-1} and δ = 4 case, compared to a value of $\sim$ 9.4 10^{-6} g cm^{-2} for the $\mathscr{F}$ = 0 (quiet-Sun) case.

The effect of nonthermal electron beam bombardment on the absolute Lc intensity can mainly be interpreted by a decrease of the departure coefficient of the hydrogen ground level (b_1) according to Eq. (1). In the absence of any nonthermal effect, the value of b_1 well exceeds unity in the upper chromosphere, owing to a significant departure from LTE. However, when there exists a nonthermal effect, the hydrogen atoms at the ground level will be greatly excited or ionized, yielding a sharp decrease of b_1. Fig. 3 plots the b_1 values for various cases shown in Fig. 2. It indicates that b_1 can be reduced by several orders of magnitude and be largely below unity. Such an effect seems to be obvious as deep as in the temperature minimum region and the upper photosphere. But this does not necessarily mean that all electron beams can penetrate so deeper. More probably, it reflects a backwarming effect caused by the enhanced Lc radiation formed above. As expected, besides the energy flux, the power index of the electron beam can also influence the magnitude of nonthermal excitation and ionization at a specific layer. However, it is interesting to note that the role of the power index is different in the upper and lower chromosphere.

Moreover, it is worthwhile to point out that the departure coefficient b_1 in the upper chromosphere can be estimated through a comparison of the Lc spectrum and the millimeter-wave continuum. At a wavelength of a few millimeters, optical depth unity occurs at approximately the same height as it does in the Lc. In principle, such a Hydrogen free-free continuum is formed in LTE. Therefore, its source function equals the Planck function (B_λ) and the emergent intensity is insensitive to the nonthermal effect. In the Lc case, however, the source function equals B_λ/b_1 and the emergent intensity depends strongly on b_1, which is very sensitive to the nonthermal effect. This argument

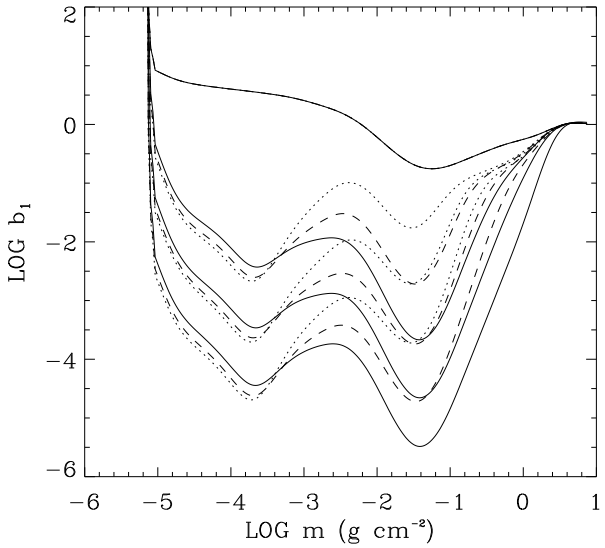

Fig. 3. Column mass distribution of the departure coefficients of the hydrogen ground level computed for the quiet-Sun model imposed by various electron beams. Solid, dashed, and dotted lines represent cases of δ = 3, 4, and 5 respectively. From top to bottom, each group of lines correspond to $\mathscr{F}$ = 0, 10^{10}, 10^{11}, and 10^{12} ergs cm^{-2} s^{-1}. Notice the overlapping of the topmost three lines for $\mathscr{F}$ = 0 (quiet-Sun case without any nonthermal effect)

has been confirmed by our computations. Closely coordinated ground-based and space-based observations would be required if we want to perform such a comparison.

While a higher chromospheric temperature, a larger coronal mass density (lower transition region), and the nonthermal effect of electron beam bombardment all contribute to increase the Lc intensity, the spectrum in the third case does show a distinguishable lower color temperature. Thus, the Lc spectra provide us a useful tool for diagnosing the nonthermal processes in solar flares, in complement to the line profile or Bc (Pc) diagnostics (e.g., Aboudarham & Hénoux 1987; Aboudarham et al. 1990; Fang et al. 1993; Hénoux et al. 1990, 1995).

It seems to be difficult to diagnose the power index of nonthermal electrons from the Lc spectrum itself, since the effect of varying the power index on the Lc intensity is less pronounced than the effect of varying the energy flux (see Fig. 2). However, the fact that the Lc and Bc are formed at quite different heights gives us a clue to use them together to infer the relative importances of the energy deposition at different layers, which are related in a large degree to the electron power index (see Fig. 3). As an example, Table 1 presents the computed Lc and Bc intensities for different power index values while the energy flux is fixed to be 10^{11} ergs cm^{-2} s^{-1}. Three cases of μ = 1.0, 0.5, and 0.2 are shown. It indicates clearly that, the larger the δ value is, the higher the Lc intensity but the lower the Bc intensity will be. Such different effects of varying the power index on the Lc and Bc intensities can be well understood considering that a harder (softer) electron beam tends to deposit more energy in the lower (upper) chromosphere where the Bc (Lc) is formed. The exception that at μ = 1.0 (disk center) the Bc intensity is insensitive to δ is only due to its deeper forming layer at which the nonthermal effect becomes less significant.

Table 1. Lc (900 Å) and Bc (3640 Å) intensities (in units of ergs cm^{-2} s^{-1} ster^{-1} Å^{-1}) computed for the quiet-Sun model imposed by electron beams with different power indices δ but a fixed energy flux $\mathscr{F}$ = 10^{11} ergs cm^{-2} s^{-1}

Continua	δ = 3	δ = 4	δ = 5
Lc (μ = 1.0)	1.15 10^4	1.81 10^4	2.23 10^4
Bc (μ = 1.0)	4.19 10^6	4.21 10^6	4.19 10^6
Lc (μ = 0.5)	1.03 10^4	1.61 10^4	1.96 10^4
Bc (μ = 0.5)	3.04 10^6	2.94 10^6	2.86 10^6
Lc (μ = 0.2)	9.21 10^3	1.42 10^4	1.73 10^4
Bc (μ = 0.2)	2.75 10^6	2.30 10^6	2.04 10^6

Note that the computation in Table 1 is based on the quiet-Sun model, thus representing roughly the situation in the early impulsive phase of flares. With the flare development, the dependence of Lc and Bc intensities on the electron power index will be changed somewhat, influenced mainly by a varying coronal mass density.

4. Conclusions

Using a program for non-LTE model computations, we have computed the Lc intensities for different flare circumstances, namely, the temperature rise in the chromosphere, the downward shift of the transition region, and the nonthermal effect of a precipitating beam of electrons. All the three factors can enhance the Lc intensity by various amounts. However, the third case produces a Lc spectrum with a significantly lower color temperature than the former two cases. It thus provides a diagnostic tool to discriminate whether the nonthermal effect plays an obvious role during solar flares. It is also suggested that the relative magnitudes of Lc and Bc enhancements can be used to infer the energy distribution type, e.g., the power index of the beam electrons. Space programs carried out recently or in the future may provide relevant observations on this topic.

Finally, we like to point out that the computational results are quite model-dependent, thus they cannot be used to explain any specific event. Our purpose is only to show the potential diagnostic role of the Lc for flare nonthermal processes. It is preferably used together with line profile diagnostics.

Acknowledgements. The authors are very grateful to M. Stix for valuable discussions, and to C. Fang for his contribution in making the computation program. Great thanks are also due to the referee, R.W. Noyes, for his helpful comments and suggestions. M.D.D. would like to thank the staff of the Kiepenheuer-Institut for their kind hospitality supporting his visit there.

References

Aboudarham J., Hénoux J.C., 1987, A&A 174, 270

Aboudarham J., Hénoux J.C., Brown J.C., et al., 1990, Solar Phys. 130, 243
Avrett E.H., 1991, Harvard-Smithsonian Center for Astrophysics Preprint Series No. 3322
Avrett E.H., Kurucz R.L., Loeser R., 1984, BAAS 16, 450
Avrett E.H., Machado M.E., Kurucz R.L., 1986, in: Neidig D.F. (ed.) The Lower Atmosphere of Solar Flares, National Solar Observatory, Sunspot, NM, p. 216
Fang C., Ding M.D., 1995, A&AS 110, 99
Fang C., Hénoux J.C., Gan W.Q., 1993, A&A 274, 917
Gan W.Q., Fang C., 1987, Solar Phys. 107, 311
Hénoux J.C., Aboudarham J., Brown J.C., et al., 1990, A&A 233, 577
Hénoux J.C., Fang C., Gan W.Q., 1995, A&A 297, 574
Machado M.E., Avrett E.H., Vernazza J.E., Noyes R.W., 1980, ApJ 242, 336
Machado M.E., Noyes R.W., 1978, Solar Phys. 59, 129
Noyes R.W., Kalkofen W., 1970, Solar Phys. 15, 120
Thompson A.M., Brown J.C., Craig I.J.D., Fulber C., 1992, A&A 265, 278
Vernazza J.E., Avrett E.H., Loeser R., 1981, ApJS 45, 635
Vernazza J.E., Noyes R.W., 1972, Solar Phys. 22, 358

This article was processed by the author using Springer-Verlag LaTeX A&A style file *L-AA* version 3./* *'